

# Non-Gaussian numerical errors versus mass hierarchy

Y. Meurice, and M.B. Oktay

*Department of Physics and Astronomy*

*The University of Iowa, Iowa City, Iowa 52242, USA*

## Abstract

We probe the numerical errors made in renormalization group calculations by varying slightly the rescaling factor of the fields and rescaling back in order to get the same (if there were no round-off errors) zero momentum 2-point function (magnetic susceptibility). The actual calculations were performed with Dyson's hierarchical model and a simplified version of it. We compare the distributions of numerical values obtained from a large sample of rescaling factors with the (Gaussian by design) distribution of a random number generator and find significant departures from the Gaussian behavior. In addition, the average value differ (robustly) from the exact answer by a quantity which is of the same order as the standard deviation. We provide a simple model in which the errors made at shorter distance have a larger weight than those made at larger distance. This model explains in part the non-Gaussian features and why the central-limit theorem does not apply.

## I. INTRODUCTION

In the standard model of electro-weak and strong interactions, all the masses are generated by couplings to a scalar Higgs particle. However, one might be inclined to think that, ultimately, gravitational interactions should be responsible for mass generation. If there is no new physics between the electro-weak scale and the Planck scale and if we know nothing about the Planck scale interactions, the best we can do is to use an effective scalar Lagrangian with a cut-off of the order of the Planck scale. In this approach, one is confronted with the hierarchy problem [1], which means that in order to keep a physical mass very small in cut-off units, one needs to fine-tune some parameter of the theory (usually the bare mass) with an incredible precision. In four dimensions, this fine-tuning can be understood in terms of perturbative quadratic divergences.

In the renormalization group (RG) approach of field theory [2], the need for fine-tuning can be related to the existence of unstable directions in a way which is independent of perturbation theory in a particular dimension. In this approach, the renormalized mass expressed in cut-off units decreases exponentially with the number of iterations spent near an unstable fixed point. In order to keep the mass small, one needs to fine-tune the initial parameter in order to start close to the critical hypersurface. This hypersurface in the space of bare Lagrangians separates the symmetric phase from the symmetry broken phase and contains the unstable fixed point.

In the following, we use the statistical mechanics language where criticality is approached by tuning the inverse temperature  $\beta$  close to its critical value  $\beta_c$ . In terms of this parameter, the ratio of the physical mass  $m$  and the ultra-violet (UV) cutoff  $\Lambda$  is

$$m/\Lambda \sim (\beta_c - \beta)^{\gamma/2}, \quad (1.1)$$

where  $\gamma$  is the critical exponent associated with the magnetic susceptibility. In four dimensions,  $\gamma = 1$ . If we take  $m = 100 \text{ GeV}$ , a typical electroweak scale, and  $\Lambda = 10^{19} \text{ GeV}$  of the order of the Planck mass, we need to fine-tune  $\beta$  with 34 digits.

The main virtue of the RG approach is to introduce some hierarchy in the information contained in the partition function. At each iteration, the information relevant to understand the large distance behavior is amplified, while the rest of the information is discarded according to its degree of irrelevance. However if some “noise” is introduced in this process, for instance as numerical errors in the calculation, the error in the relevant direction will be amplified too. This may lead to situations where the amplified errors wipe out the careful fine-tuning and one obtains meaningless results.

In this article, we discuss the numerical errors with examples where the RG transformation can be calculated for many iterations. The models used for our calculations are Dyson’s hierarchical model [3], for which very accurate methods of calculation [4,5] have been recently designed, and a simplified version [6] of this model for which the nonlinear aspects of the interpolation between fixed points is understood in great detail. For comparison, we also considered a random number generator designed to produce a Gaussian distribution.

The question of numerical errors in RG calculation has been briefly discussed in recent publications. The mechanism of error amplification was identified in section IV of Ref. [4]. In these calculations, we probed the numerical errors by slightly varying the parameter (denoted  $s$  hereafter) used to rescale the fields at each iteration of the RG transformation

and exploiting the fact that the physical quantities such as the magnetic susceptibility  $\chi$  are independent of the choice of rescaling. This procedure is reviewed in section III. We predicted that if  $\delta$  represents a typical round-off error (of the order of  $10^{-16}$  in double precision calculations), the relative difference between the numerical values obtained for two slightly different values of  $s$  should be of the order

$$\Delta\chi/\chi \sim \delta(\beta_c - \beta)^{-1} . \quad (1.2)$$

This behavior was observed in good approximation for a wide range of  $\beta$  (see Fig. 4 of Ref. [4]). A consequence of this result is that at fixed  $\delta$  and  $m$ , there is a maximum UV cutoff of the order of  $m\delta^{-\gamma/2}$  beyond which the result of a calculation becomes totally meaningless.

In the models we have considered, the exact rescaling factor  $s$  for which the RG transformation has a non-trivial fixed point (denoted  $s_{exact}$  hereafter) is *exactly* the same as for a free theory. In models with nearest neighbor interactions, this is only approximately the case. The free value is corrected whenever the critical exponent  $\eta$  is non-zero. Since in most cases,  $\eta$  is only known with a finite accuracy, one is naturally led to consider a range of values for  $s$ . In section III.b of Ref. [5] we considered the distribution of values of the susceptibility for 2000 values of  $s$ . To our surprise, we found that the errors did not average out to the correct value which was calculated using higher precision arithmetic. In addition, we found that the distribution of errors was not Gaussian. In the present paper, we readdress these questions with larger statistics and we compare the results with other models. The technical details of our analysis are outlined in section II.

Our first result is that the average error is of the same order of magnitude as the standard deviation of the distribution. There is a systematic bias in the calculations and one does not gain anything by increasing the statistics. This bias depends on the peculiarities of arithmetic round-offs and we have not attempted to model it from a “microscopic” point of view. It should however be noticed that the average error is “compiler robust” and that it should in principle be understandable at least for the simplified model for which only a few arithmetic operations are needed at each iteration of the RG transformation.

Another robust result is that all our RG calculations show significant departures from Gaussian behavior. These departures can be estimated in terms of the skewness and kurtosis coefficients. In all the RG calculations these coefficients are at least one order of magnitude larger than the corresponding quantities for the Gaussian random number generator.

How do the repeated errors fail to erase the details of the individual distribution and produce a Gaussian distribution as in the central limit theorem? We have considered two possible explanations. The first one is that the distribution of errors changes from step to step. A detailed study shows that there are indeed small variations in these distributions, however this might not be the most important effect. The main reason why the central limit does not apply seem to be that the errors are added with unequal weight. The errors made during the initial iterations are more amplified than errors made at later stage. As a consequence, the “weighted average” inherits the skewness and kurtosis of the individual distribution. Since these have “short tails”, so does the distribution of errors, unlike non-Gaussian distributions found in the study of turbulence which have “long tails”.

Our results impose limitations on numerical approaches of scalar field theory, however these are not drastic. The main result is that as far as the average of low powers of the total field is concerned, a hierarchy  $\Lambda/m$  requires a number of significant digits proportional to

$\text{Log}(\Lambda/m)$ , which is not prohibitive for  $\Lambda/m \sim 10^{17}$ .

## II. TECHNICAL OUTLINE OF THE PAPER

The renormalization group (RG) approach of scalar field theory, the hierarchy problem and our strategy to probe the numerical errors are reviewed in generic terms in section III. The specific models used for our calculations are presented in section IV.

In section V, we consider seven samples with  $10^5$  data points, six from RG calculations and one designed to produce a Gaussian distribution. It should be noted that in all cases randomness is due to sensitive dependence on the initial conditions. We show that the departure from Gaussian behavior of the distributions of RG values are significantly larger than in the case of the random number generator designed to produce a Gaussian distribution. We also show that the errors spread differently when  $s < s_{exact}$  and  $s > s_{exact}$ , indicating that the sample should be “resolved” into subsamples with different distributions.

Subsamples are analyzed quantitatively in section VI in terms of “uniformity indicators” designed to establish correlations between the values of  $s$  and the moments of the distribution. These indicators take values close to 1 when the sample is obtained from independent and identically distributed random variables. It is found that samples with only  $s < s_{exact}$  or only  $s > s_{exact}$  have much better uniformity than the the samples combining both sets of values. In the case of the simplified model, the samples with only  $s < s_{exact}$  or only  $s > s_{exact}$  have values of the indicators which seem consistent with being samples coming from independent and identically distributed random variables. For the hierarchical model, the analogous samples need further resolution.

It should be noted that in general one expects fluctuations of the order of (spread of the parent distribution)/((size of the sample)<sup>1/2</sup>). Since we use large samples, these fluctuations are expected to be small. Compared to this small scale, the variations of the estimators for  $s < s_{exact}$  and  $s > s_{exact}$  are large. However, they are still relatively small when compared to the spread itself. Consequently, it still makes sense to talk in an approximate way about, for instance, the mean of the distribution. To take an example, one can look at Table I and see that the average errors for  $s < s_{exact}$  (803) and  $s > s_{exact}$  (1297) differ by approximately one quart of the standard deviation of the any of the two samples. Consequently, we can still say that for any value of  $s$ , the error is approximately 1000. These remark should be kept in mind while we use expressions such as “the moments of a distribution”.

A specific model where the errors made during the initial iterations are more amplified than errors made at later stage is provided in section VII. In the conclusions, we discuss the limitations that our results impose on numerical approaches of scalar field theory. The situation is compared to what happens in chaotic dynamical systems and in the study of turbulence.

## III. GENERAL STRATEGY TO PROBE THE NUMERICAL ERRORS

Before getting into the specifics of model calculations, we would like to describe in general terms, our method to probe the numerical errors. The main points of this section are the following. First, the RG transformation involves a rescaling of the sum of the

fields in boxes of increasing sizes. In general, this rescaling factor is only known with a finite accuracy and so some range of values should in general be considered. Second, the physical quantities are independent of the choice of this rescaling factor. However in practical numerical calculations, the arithmetic errors are different for different choices of rescaling factor. Consequently, we can use large samples of rescaling factors to obtain a statistical distribution of these errors. We now proceed to discuss these points in the case of a generic scalar field theory.

Let us consider a scalar model in  $D$ -dimensions with a lattice spacing  $a_0$ . We first integrate the fields in blocks of side  $ba_0$  while keeping the sum of the fields in the block constant. We then divide the sums of the fields by a factor  $b^{(2+D-\eta)/2}$  and treat them as our new field variables. The procedure defines a discrete renormalization group transformation provided that the scale factor  $b$  is real number strictly larger than 1.

The critical hypersurface (in the space of bare Lagrangians) is given as the stable manifold (e.g. the basin of attraction) of a non-trivial fixed point of this transformation. The stable manifold can be reached by considering a family of models indexed by a parameter which can be tuned in order to cross the stable manifold. In field theory context, one usually pick the bare mass to accomplish this purpose. In the statistical mechanics formulation, the inverse temperature  $\beta$  can be tuned to its critical value  $\beta_c$  which is a function of the other interactions. This notation will be used later.

The information that we are keeping during the renormalization group transformation is encoded in the average values of all the integer powers of the sum of the fields in the blocks. We call these average values the “zero momentum Green’s functions at finite volume”. This set of values can be thought of as an element of an infinite vector space. Near the fixed point, we can use the eigenvectors of the linearized transformation as a basis. As far as we are close to the fixed point, the average values of the powers of the *rescaled* total field stay approximately unchanged after one transformation. However at each iteration, the components in the eigendirections are multiplied by the corresponding eigenvalue. In the following, we discuss the case where there is only one relevant direction, in other words, only one eigenvalue larger than 1. We call this eigenvalue  $\lambda$ .

After repeating the renormalization group transformation  $n$  times, we have replaced  $b^{Dn}$  sites by one site and associated a block variable with it. If at this point we neglect the interactions among the blocks of size  $b^{Dn}$  and larger, we can calculate the finite volume volume Green’s functions. For the sake of definiteness, we only discuss the case of the two point function. In the statistical mechanics language, the zero-momentum two point function is called the magnetic susceptibility. We define the finite volume susceptibility  $\chi_n$  as the average value of the square of the sum of all the (unrescaled) fields divided by the number of sites  $b^{Dn}$ .

From the above discussion, we estimate

$$\chi_n \simeq b^{n(2-\eta)}(K_1 + K_2\lambda^n(\beta_c - \beta)) \quad (3.1)$$

The power of  $b$  comes from rescaling back two powers of the fields to their original values, together with the division by the number of sites. The constant  $K_1$  is the constant value of the average of the square of the *rescaled* sum of the fields at the fixed point. The constant  $K_2$  depends on the way the critical hypersurface is approached when  $\beta$  is varied close to  $\beta_c$ .

We want to emphasize that Eq. (3.1) is valid only if the linearization procedure is

applicable, in other words if  $\lambda^n(\beta_c - \beta) \ll 1$ . On the other hand, when  $n$  reaches some critical value  $n^*$  such that

$$\lambda^{n^*}(\beta_c - \beta) \simeq 1 , \quad (3.2)$$

non-linear effects become important and the sign of  $(\beta_c - \beta)$  becomes important. In the following we will consider exclusively the case of the symmetric phase which is simpler. For a discussion in the case of the broken symmetry phase ( $\beta > \beta_c$ ), the reader may consult Ref. [7]. If  $\beta < \beta_c$ , the value of  $\chi$  starts stabilizing when  $n$  gets of the order of  $n^*$ . As a consequence,

$$\chi_\infty \sim b^{n^*(2-\eta)} \sim (\beta_c - \beta)^{-\gamma} , \quad (3.3)$$

with

$$\gamma = (2 - \eta)\ln b / \ln \lambda . \quad (3.4)$$

When  $n$  gets larger, the high-temperature fixed point is reached rapidly. This fixed point is completely attractive. The irrelevant directions are manifested by volume effects decreasing like  $b^{-n^2}$ . A model calculation of these effects can be found in Ref. [4].

For most models studied in the literature, the exact rescaling factor  $s = b^{(2+D-\eta)/2}$  is not known with perfect accuracy. For instance in a Monte Carlo calculation for values of the couplings minimizing the subleading corrections, the values of  $\eta$  obtained (for two-components in 3 dimensions) is [8] 0.0381 with errors of order 2 in the last quoted digit. Since at the end of the calculation we are rescaling back to the original field variables, this uncertainty would not affect the physical results provided that we were able to carry the integrations exactly. If the integrations are carried numerically, the arithmetic operations are performed differently and choosing a sample of values for the rescaling factor  $s$  close to the approximate values can be used to obtain a statistical sample of the numerical errors.

We will thus consider values of the rescaling factor  $s$  of the form  $s_{exact} + \delta$ , where  $s_{exact}$  is the value for which there is an exact fixed point. In some sense  $\delta$  can be seen as the “seed” of a random number generator. We will now perform sample calculations for two models and compare our results with the results obtained from a set of seeds for a random number generator designed to produce approximate Gaussian distributions.

## IV. MODEL CALCULATIONS

In this section, we describe in detail the three procedures used to obtain the data analyzed in the following sections. We discuss the hierarchical model [3] (subsection A), a simplified version [6] of it (subsection B) and a random number generator which represents our naive expectations for the two other cases (subsection C).

### A. The hierarchical model

The choice of the hierarchical model allows easy calculations with a controllable accuracy. In order to avoid repetitions, we refer the reader to Ref. [4] for a more systematic

presentation. The main interest of this model is that only the local potential (or equivalently, the part of the measure which factorizes into a product of identical local functions which are called “the local measure” later) is affected by the RG transformation while the “kinetic” part is left invariant.

The block-spin procedure can then be summarized by a simple integral formula (Eq. (2.2) in Ref. [4]) for the local measure. Taking the Fourier transform and rescaling the sum of the fields in the block by an *arbitrary* rescaling factor  $1/s$  one obtains [4] the recursion relation

$$R_{n+1}(k) = C_{n+1} \exp\left(-\frac{1}{2}\beta\left(\frac{c}{4}s^2\right)^{n+1} \frac{\partial^2}{\partial k^2}\right) \left(R_n\left(\frac{k}{s}\right)\right)^2. \quad (4.1)$$

The parameter  $c$  is set equal to  $2^{1-2/D}$  in order to approximate a  $D$ -dimensional model with nearest neighbor interactions. In the following the value  $D = 3$  will be used.

We fix the normalization constant  $C_n$  in such way that  $R_n(0) = 1$ .  $R_n(k)$  has then a direct probabilistic interpretation. If we call  $M_n$  the total field  $\sum \phi_x$  inside blocks of side  $2^n$  and  $\langle \dots \rangle_n$  the average calculated without taking into account the interactions among different blocks of this size find

$$R_n(k) = \sum_{q=0}^{\infty} \frac{(-ik)^{2q}}{2q!} \frac{\langle (M_n)^{2q} \rangle_n}{s^{2qn}} \quad (4.2)$$

We see that the Fourier transform of the local measure after  $n$  iterations generates the zero-momentum Green’s functions calculated with  $2^n$  sites. In particular, we are interested in calculating the finite volume susceptibility

$$\chi_n = \frac{\langle (M_n)^2 \rangle_n}{2^n} = -2a_{n,1} \left(\frac{s^2}{2}\right)^n. \quad (4.3)$$

As far as we are only interested in the calculation of  $\langle (M_n)^{2q} \rangle_n$ , the choice of  $s$  is a matter of convenience. For the calculations in the high temperature phase (symmetric phase) not too close to the critical points, or high temperature expansions the choice  $s = \sqrt{2}$  is natural [9]. On the other hand, the choice of rescaling factor  $s = 2c^{-1/2}$  makes the explicit dependence on  $n$  in Eq. (4.1) disappear. For any other value of  $s$ , the map is somehow analogous to a differential equation with explicitly time-dependent coefficients. What we call “the RG transformation” in section III, is Eq. (4.1) with  $s = 2c^{-1/2}$ . It corresponds to the values  $b = 2^{1/D}$ ,  $\eta = 0$  and  $s = b^{(2+D)/2}$  of the parameters defined in section III. For this value of  $s$ , Eq. (4.1) has non-trivial fixed point [10] which seems to be unique [5].

We have calculated the susceptibility for the Ising measure ( $R_0(k) = \cos(k)$ ) with  $D = 3$  (i.e.  $c = 2^{1/3}$ ) and  $\beta = \beta_c - 10^{-8}$ . The calculations have been performed using double precision Fortran. Using the approximate error given in Eq. (1.2), we see that 8 out of the 16 significant digits of  $\chi$  should be correct for  $\beta = \beta_c - 10^{-8}$ . Since we are in the high-temperature phase,  $\chi_n$  stops growing after approximately  $n^* \simeq 52$  iterations (see section III and Ref. [5] for details). The 16 digits of  $\chi_n$  are completely stabilized after  $n = 140$  iterations. We call this stable value  $\chi(s)$  where  $s$  refers to the value of  $s$  in Eq. (4.1) used for the numerical calculation. The calculations have performed using dimensional approximations of degree  $l_{max}$ :

$$R_n(k) = 1 + a_{n,1}k^2 + a_{n,2}k^4 + \dots + a_{n,l_{max}}k^{2l_{max}} , \quad (4.4)$$

for which the recursion formula for the  $a_{n,m}$  reads :

$$a_{n+1,m} = \frac{\sum_{l=m}^{l_{max}} (\sum_{p+q=l} a_{n,p}a_{n,q}) [(2l)!/(l-m)!(2m)!] (c/4)^l [-(1/2)\beta]^{l-m}}{\sum_{l=0}^{l_{max}} (\sum_{p+q=l} a_{n,p}a_{n,q}) [(2l)!/l!] (c/4)^l [-(1/2)\beta]^l} \quad (4.5)$$

We found that the 16 digits of  $\chi_n$  were completely stabilized for  $l_{max} = 50$ .

We have used the set of values  $s = 2/\sqrt{c} \pm m \times 10^{-8}$  with  $m = 1, \dots, 10^5$ . We recorded the difference of  $\chi(s)$  defined above with respect to the accurate value  $\chi = 5.2316268857268 \times 10^{10}$ . This value was obtained by performing the calculation using higher precision arithmetic (namely 30 digits). We have checked that this accurate result is insensitive to changes in  $s$ . The results are discussed in the next sections.

## B. A simplified model

As noticed in Ref. [4], for  $\beta < \beta_c$  and  $n \gg n^*$  Eq. (4.1) implies the approximate behavior

$$\chi_{n+1} \simeq \chi_n + (\beta/4)(c/2)^{n+1} \chi_n^2 . \quad (4.6)$$

This map has been studied [6] on its own in the rescaled form

$$h_{n+1} = (c/2)h_n + (1 - c/2)h_n^2 . \quad (4.7)$$

This map can be seen as a drastically simplified version of the hierarchical model. One can check that if  $0 \leq h_0 \leq 1$ ,  $\lim_{n \rightarrow \infty} (2/c)^n h_n$  is finite. This limit plays the role of the susceptibility in the following and can be calculated accurately by combining dual expansions [6].

Eq. (4.7) has an unstable fixed point at  $h = 1$  with eigenvalue  $\lambda = 2 - c/2$ . We have required  $\lambda = 1.427$ , approximately as for the hierarchical model with  $D = 3$ , in order to keep the value of  $n^*$  the same. Consequently, the value of  $c$  used in Eq. (4.7) is *not* the same as the value of  $c$  for the hierarchical model with  $D = 3$ .

We have introduced the rescaling factor  $s$  through the redefinition

$$a_n \equiv (s^2 c/4)^{-n} h_n , \quad (4.8)$$

in terms of which the map becomes

$$a_{n+1} = (2/s^2)a_n + (1 - c/2)(s^2 c/4)^{n-1} a_n^2 \quad (4.9)$$

After calculating,  $a_n$  one can always return to  $h_n$  using Eq. (4.8). If we had the chance to use exact arithmetic the expression would be independent of  $s$ .

We have performed calculations for  $h_0 = a_0 = 1 - 10^{-8}$ . We found that 150 iterations were sufficient to stabilize  $\lim_{n \rightarrow \infty} (2/c)^n h_n$ . We have calculated this value for  $s = 2/\sqrt{c} \pm m \times 10^{-8}$  with  $m = 1, \dots, 10^5$ , as in the previous case. We have then subtracted the more accurate value

$$\lim_{n \rightarrow \infty} (2/c)^n h_n = 3.842965603774557 \times 10^{12} . \quad (4.10)$$

obtained and checked exactly with the same procedure as in the previous subsection.



### C. A model with gaussian distribution

In order to provide a comparison of the errors distributions of the two previous models, we have also generated  $10^5$  numbers using a method designed to give a gaussian distribution. Since in the two previous cases we have approximately  $n^* = 52$  random processes before the value recorded starts stabilizing, we have added 52 random numbers. These random numbers have been produced by using repeated multiplication by a large number ( $7^5$ ) followed by a reduction modulo 1 (in other words, we drop the integer part). This procedure is inspired by results reviewed in Ref. [11]. Iterating this procedure, we generate a sequence of random numbers which we expect to be uniformly distributed between 0 and 1. In order to get numbers distributed between -1 and 1, we multiply each number by 2 and subtract 1. Finally, in order to get numbers approximately of the same order as the numbers of the other two sets, we have multiplied the final sum of 52 random numbers by 1000. The final results depends only on the initial number provided (the “seed”). We have repeated this calculation for  $10^5$  values of the seed between 0 and 1.

The above discussion can be summarized as follows. We iterate 52 times the map

$$\alpha_{n+1} = 7^5 \alpha_n \text{ Modulo } 1, \quad (4.11)$$

and then calculate

$$X_j = 1000 \times \sum_{n=1}^{52} (2\alpha_n - 1) . \quad (4.12)$$

The sub-index  $j$  corresponds to different values of the seed  $\alpha_0$ . The data analyzed in the next sections corresponds the choice

$$\alpha_0(j) = j/100005.23 , \quad (4.13)$$

with  $j = 1, \dots, 10^5$ . The choice of the denominator is motivated by the fact that we want a spacing between successive initial values slightly smaller than  $10^{-5}$ . The decimal points (.23) have been adjusted empirically in order to get a good uniformity of in subsamples (this question is discussed in section VIB).

The map of Eq. (4.11) is designed to provide a sample from a variable  $\alpha$  which we expect to be uniformly distributed between 0 and 1. If this is the case, we should have  $\langle(2\alpha - 1)\rangle = 0$  and  $\text{Var}(2\alpha - 1) = 1/3$ . We use the common notation  $\text{Var}(A) = \langle(A - \langle A \rangle)^2\rangle$ . If we now define,  $X = 1000 \times \sum_{n=1}^{52} (2\alpha_n - 1)$ , we expect

$$\begin{aligned} \langle X \rangle &= 0 ; \\ \text{Var}(X) &= (1000)^2 \times (52/3) \simeq (4163)^2 . \end{aligned} \quad (4.14)$$

These predictions will be tested in section VI.

## V. ERROR DISTRIBUTIONS

In order to get a first idea about what can be done to characterize the distributions of values obtained by the procedures described in the previous section, we first consider the

hierarchical model and display a subsample of 1000 data points for  $s$  below  $s_{exact} = 2/\sqrt{c}$  and 1000 data points for  $s$  above this value. The selection of the subsample was done by taking one out of every 100 values out of the original sample. More precisely, the integer  $m$  used in the parametrization of  $s$  given in subsection IV A, takes only values which are multiples of 100. The distribution of values is shown in Fig. 1.

One immediately realizes that the distribution is not symmetric about  $s = 2/\sqrt{c}$ . If  $s > 2/\sqrt{c}$ , the values of  $\chi$  are more spread than if  $s < 2/\sqrt{c}$ . An histogram can be obtained by dividing the data points into “horizontal bins” of equal vertical height and counting the number of data points in each bin. This procedure has been followed for 50,000 data points with  $s > 2/\sqrt{c}$  and 50,000 data points with  $s < 2/\sqrt{c}$ . Each of the two sets is obtained by taking every other point out of the data for the hierarchical model described in the previous section. With this procedure the total number of data points is still  $10^5$  and the statistical properties can be easily compared with the other samples of  $10^5$  data points. The histogram is displayed in Fig. 2.

The solid line is obtained by plugging the estimated mean and standard deviation (discussed in the next section) in a gaussian probability distribution. In the rest of this section, the terminology “Gaussian fit” refers to this procedure. One sees that there are large deviations from the Gaussian fit. Given the size of the sample it is very unlikely that the deviations can be interpreted as statistical fluctuations.

For comparison, we give in Fig. 3 an histogram of the distribution of  $10^5$  data points obtained from the random number generator discussed in section IV C. The features of the distribution can be seen better by plotting the logarithm of the number of data points in each bin. In this semi-log plot, the fit corresponding to a Gaussian distribution is simply a parabola. Also, we will study separately, the data points with  $s < 2/\sqrt{c}$  and  $s > 2/\sqrt{c}$  since from Fig. 1 they have manifestly different standard deviations. The results for the two sets of  $10^5$  data points described in subsection IV A for the hierarchical model are shown in Fig. 4.

These distributions are roughly of rectangular shape with slow modulations on the “flat” part. They can be compared with a similar graph for the random number generator (Fig. 5). On this graph, the departure from the parabolic behavior is barely visible except in the tails. Obviously, bins with zero data points cannot be shown in such a graph.

Finally, we have displayed the results for the two sets of  $10^5$  data points described in subsection IV B for the toy model (Fig. 6). One sees that significant deviations from the Gaussian fit appear in the tails. The fact that the probability distribution falls more rapidly in this region is indicative of a probability distribution of the form  $\exp(-ax^2 - bx^4)$  with  $a$  and  $b$  positive. This relative simplicity suggests that we have a better chance to fully understand this simplified example.

## VI. MOMENT ANALYSIS

### A. Moment estimators

A probability distribution is characterized by its moments. We would like to estimate the first moments of the distributions described in the previous sections *assuming* that they

are sample of a unique probability distribution. Let  $X_i$  with  $i, \dots, N$  be a set of independent and identically distributed (i.i.d.) random variables with moments

$$\begin{aligned} \langle X_i \rangle &= \mu ; \\ \langle (X_i - \mu)^r \rangle &= \mu_r , r \geq 2 , \end{aligned} \tag{6.1}$$

identical for any  $i$ . In particular,  $\mu_2 = \sigma^2$  is the variance or the square of the standard deviation  $\sigma$ . We define the estimators

$$\begin{aligned} \hat{\mu} &= (1/N) \sum_1^N X_i ; \\ \hat{\mu}_r &= (1/N) \sum_1^N (X_i - \hat{\mu})^r , r \geq 2 . \end{aligned} \tag{6.2}$$

Using the hypothesis that the random variables are independent, we can factor the powers of a given  $X_i$  and calculate its average independently. For instance, if  $i \neq j$ ,  $\langle X_i X_j \rangle = \langle X_i \rangle \langle X_j \rangle$ . Using the hypothesis that the random variables are identically distributed, we can use Eq. (6.2) to express these expectations in terms of the common values of their moments. Using these rules, one obtains

$$\langle \hat{\mu} \rangle = \mu ; \tag{6.3}$$

$$\langle \hat{\mu}_r \rangle = \mu_r + O(1/N) , r \geq 2 . \tag{6.4}$$

The biases of the  $\mu_r$  are of order  $1/N$ . It is not difficult to remove the bias, however since we will work with large samples, the corrections are very small.

In Table I, we give the estimated values of  $\mu$  and  $\sigma$  for the distributions discussed before. The abbreviation a. is short for ‘‘above’’ which means the  $10^5$  points with  $s > 2/\sqrt{c}$  for the hierarchical model (H.M.) or the toy model (T.M.). Similarly b. is short for ‘‘below’’ ( $s < 2/\sqrt{c}$ ), while a.+b. means ‘‘above and below’’ which is short for  $10^5$  points obtained by taking every other value in the ‘‘above’’ and ‘‘below’’ set as explained at the beginning of section V. Finally, ‘‘R.N.G.’’ is short for the random number generator described in subsection IV C. These notations will be used again in the following. We emphasize that a.+b. is *not* the union of a. and b. (so  $\mu_{a.+b.} \neq (1/2)(\mu_a. + \mu_b.)$ ) and that all the samples have  $10^5$  data points.

Initially we expected that  $\mu$  would be of order  $\sigma/\sqrt{N}$ . However, this is only the case for the random number generator. In all the other cases,  $\mu$ , which we remind is the average difference with respect to the accurate value, is of the same order of magnitude as  $\sigma$ . In other words, it seems impossible to get rid of the errors by using large statistics!

In order to check the compiler-dependence of our results, we have repeated the calculations of the toy model in C, Mathematica and a different version of Fortran. We found that  $\mu$  was only affected by less than 10 percent. On the other hand,  $\sigma$  varied much more significantly.

Note also that in the case of the R.N.G., the estimated value of  $\sigma$  is close to the result (4163) obtained in Eq. (4.15) by assuming that the  $\alpha_l$  are uniform over the interval  $[0, 1]$ .

As expected, the  $\sigma$  ‘‘above’’ and ‘‘below’’ are significantly different. It is very unlikely that the data ‘‘above and below’’ is a sample from a unique distribution. More generally, one could study subsamples and check that the fluctuations are compatible with their size. This is the topic of the next subsection.

## B. Fluctuations and uniformity

In the previous subsection, we have used moments estimators which are in good approximations unbiased. However, it is not clear that the sample comes from a unique distribution. One way to tackle this question is to consider the estimators in many subsamples and decide if the the fluctuations of the estimated values of the moments in the subsamples are compatible with the variance of the estimator which we now proceed to estimate.

Using again the hypothesis of independent and identical distributions, we find in leading order in  $1/N$  (in other words, up to  $O(1/N^2)$  corrections) that:

$$\text{Var}(\widehat{\mu}) = (1/N)(\mu_2) ; \quad (6.5)$$

$$\text{Var}(\widehat{\mu}_2) = (1/N)(\mu_4 - \mu_2^2) ; \quad (6.6)$$

$$\text{Var}(\widehat{\mu}_3) = (1/N)(\mu_6 - \mu_3^2 + 9\mu_2^3 - 6\mu_2\mu_4) ; \quad (6.7)$$

$$\text{Var}(\widehat{\mu}_4) = (1/N)(\mu_8 - \mu_4^2 + 16\mu_2\mu_3^2 - 8\mu_3\mu_5) . \quad (6.8)$$

The proof of these results can be found for instance in Ref. [12].

We considered the seven sets of  $10^5$  data points discussed in the previous subsection. Each set has been divided into  $m$  subsets with  $N_B$  data points. Obviously,  $N = m \times N_B$ . The partition has been done by putting together successive values of  $s$ . If one refers to Fig. 1, the subsets are vertical partitions. We call  $\widehat{\mu}_{r,S}$  (or  $\widehat{\mu}_S$ ) the estimator of  $\mu_r$  (or  $\mu$ ) in the  $S$ -th subsample. These are defined as in Eq. (6.2), except for the fact that  $N$  needs to be replaced by  $N_B$ . In order to avoid confusion, we have used a subscript  $T$  (short for Total) to designate the estimators in the whole sample. We have studied the differences between the subsample estimates and the whole sample estimates. In order to get comparable answers, we have expressed these differences in “natural units”. These units should be such that if we had a sample from a unique distribution, all the fluctuations would be of order 1. From the expressions of the variances, ones sees that  $\sigma^r/\sqrt{N_B}$  are natural units for the fluctuations of  $\widehat{\mu}_{r,S}$ . In practice, we have to replace  $\sigma$  by its estimated value. As an illustration, we have taken three sets previously abbreviated as H.M.a.+b., T.M.a.+b. and R.N.G. and divided them into  $m = 400$  sub-bins. These sub-bins are ordered according to increasing values of  $s$ . For illustration, we have displayed the fluctuations of the second moment in natural units. The results are shown in Fig. 7.

One sees that for the first two sets, there is a “jump” at  $s = 2/\sqrt{c}$  that is significantly larger than the other fluctuations. Note that we have checked that both a.+b. sets had their sub-bins ordered in the same way. Besides these jumps, the fluctuations appear to be of much more “normal” size. In order to make this visual impression quantitative, we have defined the average of the square of the fluctuations in the subsamples:

$$U_1 = (1/m) \sum_{S=1}^m (\widehat{\mu}_S - \widehat{\mu}_T)^2 ;$$

$$U_r = (1/m) \sum_{S=1}^m (\widehat{\mu}_{r,S} - \widehat{\mu}_{r,T})^2 . \quad (6.9)$$

If the sample comes from a single distribution, we expect these quantities to be equal to the variance of the corresponding estimator with fluctuations of order  $1/\sqrt{m}$ . We have thus defined some “indicators of uniformity” as

$$\begin{aligned}
p_1 &= U_1/\text{Var}(\widehat{\mu}_S) ; \\
p_r &= U_r/\text{Var}(\widehat{\mu}_{r,S}) .
\end{aligned}
\tag{6.10}$$

If the sample comes from a single distributions, the  $p_i$  should be close to 1, while a large value indicates the presence of several distributions. The values of these indicators are given for the seven sets of data points previously described in Table II.

First, one notices that the R.N.G. data has all the  $p_i$  within less than ten percent of 1. On the other hand, both a.+b. sets have large values. For the toy model, the separation into above and below is sufficient to get rid of these large values. The values for T.M.a. and T.M.b are within 20 percent of 1. This seems in good approximation compatible with a single distribution. This quantitative analysis confirms the visual impression that one gets from Figs. 4 and 6. On the other hand, it is possible to further “resolve” the a. and b. data for the hierarchical model.

In the case of the hierarchical model, the local analysis of the sub-samples shows that the rapid variations of the mean has “large-scale” tendencies. Namely we observed regions of  $s$  where in average, the mean grows linearly when  $s$  increases followed by regions where it decreases. This behavior is presently under study.

### C. Departure from Gaussian behavior

In section V, we noticed that the distributions for the toy model a. and b. were more sharply peaked than a Gaussian distribution. This feature can be analyzed more quantitatively by estimating the skewness coefficient  $\mu_3/\mu_2^{3/2}$  and the coefficient of kurtosis  $\mu_4/\mu_2^2 - 3$ . For a Gaussian distribution, both coefficients are zero. These estimations of these coefficients for the data sets previously considered are given in Table III.

For the T.M. a. and b., both coefficients are an order of magnitude larger than the corresponding coefficients for the R.N.G. . Larger deviations are observed for the other sets reflecting the lack of uniformity of these sets of data.

In summary, the above table supports the general statement that the numerical errors appearing in RG calculations are non-Gaussian. We will now attempt to explain this general feature with a simple model.

## VII. A MODEL FOR NON-GAUSSIAN ERRORS

One reason to be inclined to believe *a-priori* that errors distributions should be Gaussian is the famous central-limit theorem which asserts that the average of  $N$  i.i.d. random variables approaches a Gaussian distribution when  $N$  becomes infinite. In this section, we give an heuristic derivation of this theorem and then present a mechanism by which we can avoid ending up with Gaussian distributions.

### A. The central limit theorem

We first review the central-limit theorem in terms of a moment analysis. Let  $\alpha_j$   $j = 1, \dots, n$  be a set of i.i.d. random variables with arbitrary moments  $(\mu, \mu_2 = \sigma^2, \mu_3 \dots)$ . We

define

$$Z = [(1/n) \sum_{j=1}^n (\alpha_j - \mu)] / (\sigma/\sqrt{n}) . \quad (7.1)$$

It is clear that  $Z$  has  $\mu = 0$  and  $\sigma = 1$ . The central-limit asserts that

$$\text{Lim}_{n \rightarrow \infty} P(Z) = (1/\sqrt{2\pi}) e^{-Z^2/2} . \quad (7.2)$$

This theorem can be proven by showing that the moments of  $Z$  coincide with the moments of a normal Gaussian :

$$\mu_{2r} = (2r - 1)!! ; \quad (7.3)$$

$$\mu_{2r+1} = 0 . \quad (7.4)$$

The calculation of the expected values of  $Z^q$  goes as follows. Each term of  $Z^q$  is a product of  $q$  terms of the form  $(\alpha_i - \mu)$ . The expected value can be factored into products involving the same  $i$  and then expressed in terms of the moments. Since  $\langle \alpha_i - \mu \rangle = 0$ , each  $i$  should be repeated at least twice. For  $Z^3$ , the three  $i$  should be the same or one will be “left alone” (which would imply a vanishing average). Since the three indices have to be the same and since there are  $n$  indices we get a combinatoric factor  $n$  which is insufficient to overcome the  $n^{-3/2}$  appearing in  $Z^3$ . A similar reasoning in the case of  $Z^4$ , shows there are three ways to arrange four indices into two pairs having the same index (assuming that the index of the two pairs are distinct). If we require that the four indexes are the same, it costs an additional  $1/n$  suppression. In summary, when  $n$  becomes large

$$\langle Z^3 \rangle = n\mu_3 / (\sigma^3 n^{3/2}) - > 0 ; \quad (7.5)$$

$$\langle Z^4 \rangle = (n\mu_4 + 3n(n-1)\sigma^4) / (\sigma^4 n^2) - > 3 . \quad (7.6)$$

The argument generalizes easily, and one realizes that the odd moments vanish and the even moment reduce to the number of unordered pairs, in agreement with Eq. (7.3).

## B. Evading the central limit

In order to see how the central-limit can be evaded, we have constructed a simplified model for the numerical errors. In the rest of this section, when we say “the quantity we are calculating numerically” this means the  $R_n(k)$  function defined in Eq. (4.1) for the hierarchical model or the quantity  $a_n$  of Eq. (4.9) for the toy model. While we are near the fixed point, the numerical values appearing in these quantities which are relevant for our discussion are roughly of order 1.

We first assume that the initial data ( $R_0$  or  $a_0$ ) has an error  $\mathcal{E}_0$  in the unstable direction. Using the linearized model of section III, we see from Eq. (3.1) that as far as we are near the fixed point, the quantity we are calculating numerically is of order  $K_1$ . After one iteration,  $\mathcal{E}_0$  is amplified by a factor  $\lambda$ . In addition, an error of order  $K_1 10^{-16}$  is made. We express our ignorance about the details of the round-off errors in terms of a random variable  $\alpha_1$  which takes positive or negative values of order 1 and write the new error as  $K_1 \alpha_1 10^{-16}$ . Putting the two terms we get

$$\mathcal{E}_1 = \lambda \mathcal{E}_0 + K_1 \alpha_1 10^{-16} . \quad (7.7)$$

Iterating  $n$  times, we get

$$\mathcal{E}_n = K_1 \left( \sum_{j=0}^n \lambda^{n-j} \alpha_j \right) 10^{-16} . \quad (7.8)$$

In order to have compact notations, we have introduced a random variable  $\alpha_0$  such that  $\mathcal{E}_0 = K_1 \alpha_0 10^{-16}$ . This term is not very important for the rest of the discussion, we might have set  $\mathcal{E}_0 = 0$  and considered errors for a given initial data expressed with a finite precision. In that case, the sum in Eq. (7.8) would run from 1 to  $n$ .

The main difference between the expression of the error of Eq. (7.8) and the variable  $Z$  introduced in the discussion of the central-limit theorem, is that the  $\alpha_i$  appear with different weights. One can then escape the ‘‘pair dominance’’ mechanism which puts all the individual errors on the same footing. Instead, the short-distance errors (small  $n$ ) are more amplified than the large-distance errors (large  $n$ ). Consequently, the total error is likely to inherit some of the features of the individual errors. This intuitive picture is confirmed by an explicit calculation that we now proceed to explain.

We will calculate the skewness and kurtosis associated with

$$Y = \sum_{j=0}^n \lambda^{n-j} \alpha_j , \quad (7.9)$$

assuming that all the  $\alpha_i$  are independent and identically distributed. A detailed study of the errors associated with one iteration of the RG transformation for the toy model shows that this assumption is not totally correct but that it is a reasonable first-order approximation. A simple calculation shows that after neglecting terms of order 1 compared to  $\lambda^n$ , we obtain

$$\langle (Y - \langle Y \rangle)^3 \rangle / (\langle (Y - \langle Y \rangle)^2 \rangle)^{3/2} \simeq [(\lambda^2 - 1)^{3/2} / (\lambda^3 - 1)] (\mu^3 / \sigma^{3/2}) ; \quad (7.10)$$

$$\langle (Y - \langle Y \rangle)^4 \rangle / (\langle (Y - \langle Y \rangle)^2 \rangle)^2 - 3 \simeq [(\lambda^2 - 1)^2 / (\lambda^4 - 1)] [(\mu^4 / \sigma^4) - 3] . \quad (7.11)$$

One sees that  $Y$  inherits the non-Gaussian behavior of the  $\alpha$ 's, in the sense that the skewness and kurtosis coefficients of  $Y$  are proportional to those of  $\alpha$ .

For  $\lambda = 1.427$  and  $\alpha$  uniformly distributed between -1 and 1 (corresponding to an error of  $\pm 1$  in the last significant digit) and which is roughly what we observed for the toy model, the skewness and kurtosis coefficients of  $Y$  are 0 and -0.41 respectively. These numbers are consistent with the values obtained for the toy model. A more detailed study shows that if we replace the average in Eq. (4.12) for the random number generator by a weighted average as in Eq. (7.8), one obtains histograms very similar to those of T.M. a. or b. (see Fig. 6).

## VIII. CONCLUSIONS

We have shown that in RG calculations, perturbations occurring at different scales fail to average each other out and that the final result is most affected by the peculiarities of the short-distance perturbations. In our study the perturbations are ‘‘anthropomorphic’’ in the sense that they are due to our calculation procedure rather than to natural phenomena. We

have also shown that it is not possible to get rid of the effects by averaging over calculations at slightly different values of the rescaling parameter  $s$  (which is not known exactly in most realistic situations). The only way the errors can be reduced to an acceptable level is by using enough significant digits in the arithmetic used in the calculations.

The situation is somehow similar to what occurs in chaotic dynamical systems. There, the sensitive dependence on the initial conditions, implies that for time scales large compared to the inverse Lyapounov's exponents, one needs more significant digits than possibly achievable in order to keep track of a particular orbit. In the calculations performed here, the product of the inverse Lyapounov exponent ( $\log(\lambda)$ ) and the time of calculation ( $n^*$ ) grows only like  $(2/\gamma)\log(\Lambda/m)$  and one can obtain reasonably precise calculations of the renormalized mass with  $(\Lambda/m) \sim 10^{17}$  by using only 40 significant digits (for  $\gamma = 1$ ). If we are interested in calculating the connected higher point functions, more digits are necessary because some digits are lost in the subtraction procedure as explained in Ref. [4]. In conclusion, we see that if we are interested in the lowest point connected functions and if we have hierarchies of only 17 order of magnitudes, there is no serious limitation in our capability to calculate using the RG method.

Finally, it should be noted that non-Gaussian distributions are a common feature in the study of turbulence [13]. A simple example is the distribution of transverse velocity increments between two points separated by a distance  $l$  in a turbulent jet, denoted  $\delta v_{\perp}(l)$ . Typically, the distribution starts developing "long tails" when  $l$  becomes sufficiently small. In the case studied here, we have the opposite effect: our distribution has "short tails". This is due to the fact that the "microscopic" errors are the individual round-offs which have no tails at all.

## ACKNOWLEDGMENTS

This research was supported in part by the Department of Energy under Contract No. FG02-91ER40664. We thank A. Bhattacharjee and J. Scudder for discussions on non-Gaussian distributions.



## REFERENCES

- [1] L. Susskind, Phys. Rev. D **20**, 2619 (1979).
- [2] K. Wilson, Phys. Rev. B **4**, 3185 (1971) ; Phys. Rev. D **3**, 1818 (1971); K. Wilson and J. Kogut Phys. Rep. **12**, 75 (1974); K.Wilson, Phys. Rev. D **6**, 419 (1972).
- [3] F. Dyson, Comm. Math. Phys. **12**, 91 (1969) ; G. Baker, Phys. Rev. B**5**, 2622 (1972).
- [4] J. J. Godina, Y. Meurice, B. Oktay and S. Niermann, Phys. Rev. D **57**, 6326 (1998).
- [5] J. J. Godina, Y. Meurice, B. Oktay, Phys. Rev. D **57**, R6581 (1998); Rev. D **59**, 096002 (1999).
- [6] Y. Meurice and S. Niermann, Phys. Rev. E **60**, 2612 (1999)
- [7] J. J. Godina, Y. Meurice, B. Oktay, Phys. Rev. D **61** 1145xx-1 (in press).
- [8] M. Hasenbusch and T. Torok, Humboldt Univ. Preprint HUB-EP 99/18; cond-mat/9904408.
- [9] Y. Meurice, G. Ordaz and V. G. J. Rodgers, Phys. Rev. Lett. **75**, 4555 (1995). Y. Meurice, S. Niermann, and G. Ordaz, J. Stat. Phys. **87**, 363 (1997).
- [10] H. Koch and P. Wittwer, Math. Phys. Electr. Jour. (<http://mpej.unige.ch/>), **1**, Paper 6 (1995).
- [11] W. Press, S. Teukolsky, W. Vetterling and B. Flattery, *Numerical Recipes in C*, Second Edition, (Cambridge University Press, Cambridge, 1992), p. 278.
- [12] M. Kendall and A. Stuart, *The Advanced Theory of Statistics* (Charles Griffin, London, 1977).
- [13] U. Frish, *Turbulence* (Cambridge University Press, Cambridge, 1995); Chapter 8.

FIGURES

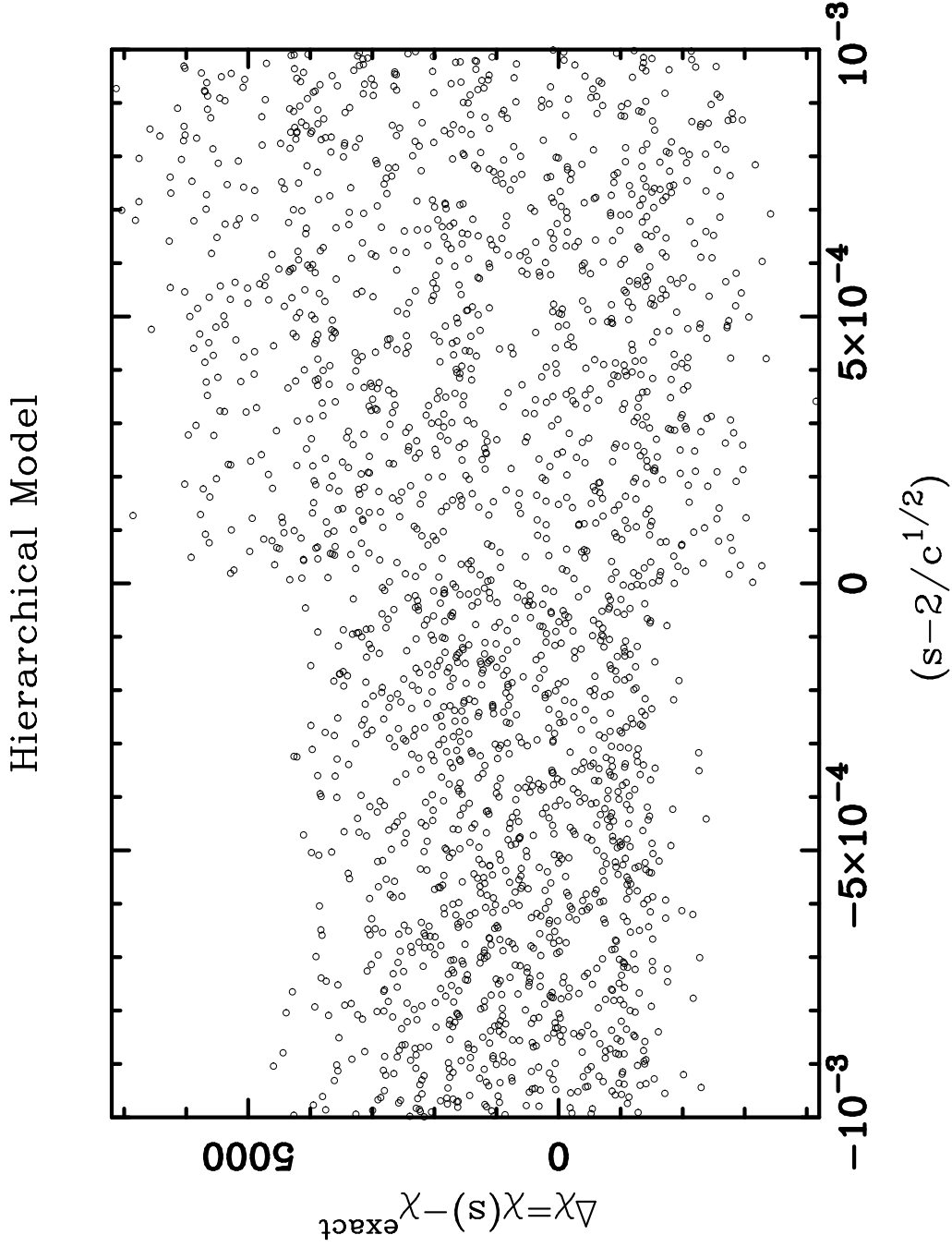


FIG. 1. Distribution of  $\chi(s) - \chi^{exact}$  for the hierarchical model for various values of the rescaling variable  $s$ .

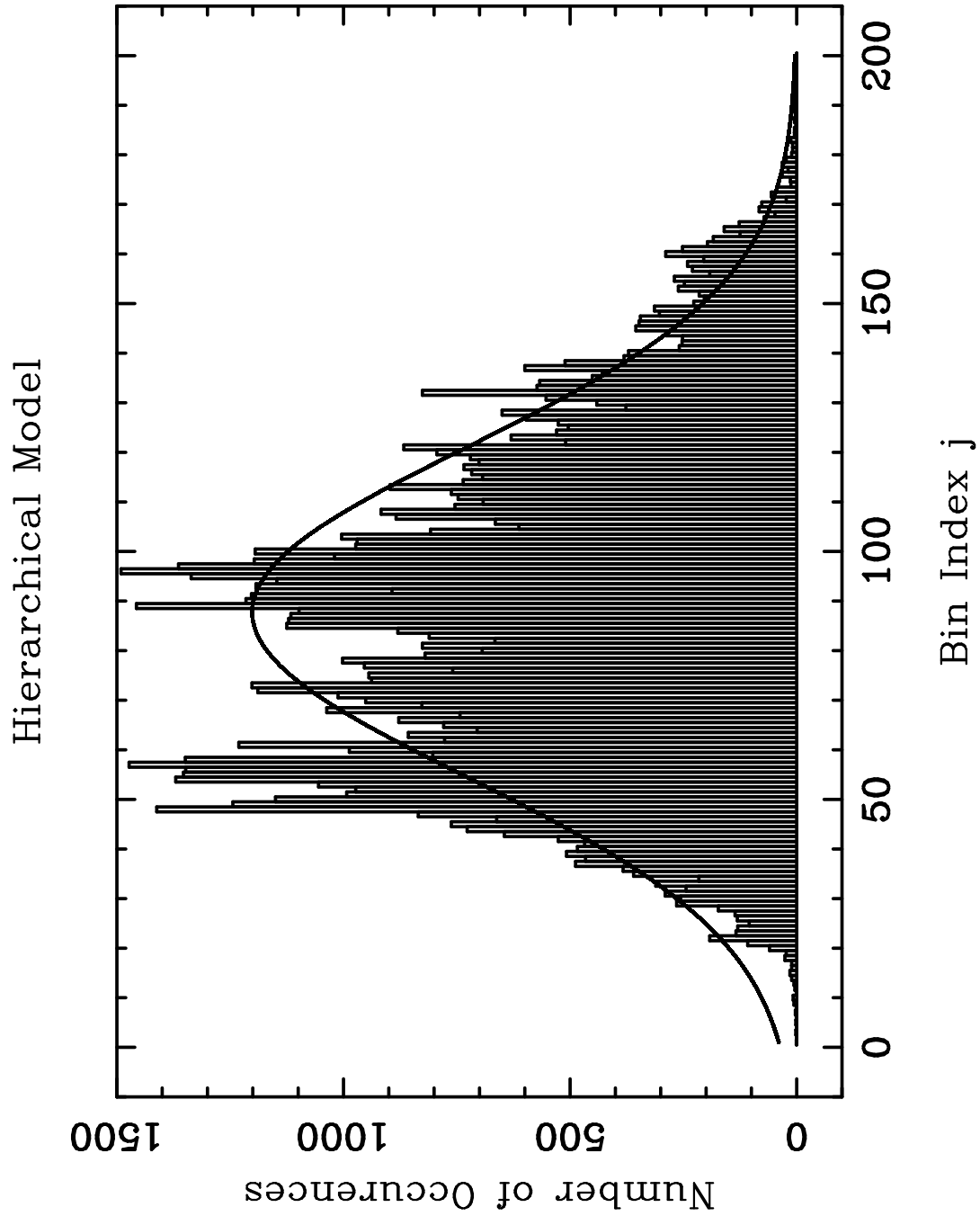


FIG. 2. Partition of the  $10^5$  values of  $\chi(s)$  into 200 bins as described in the text. The solid line is a gaussian fit.

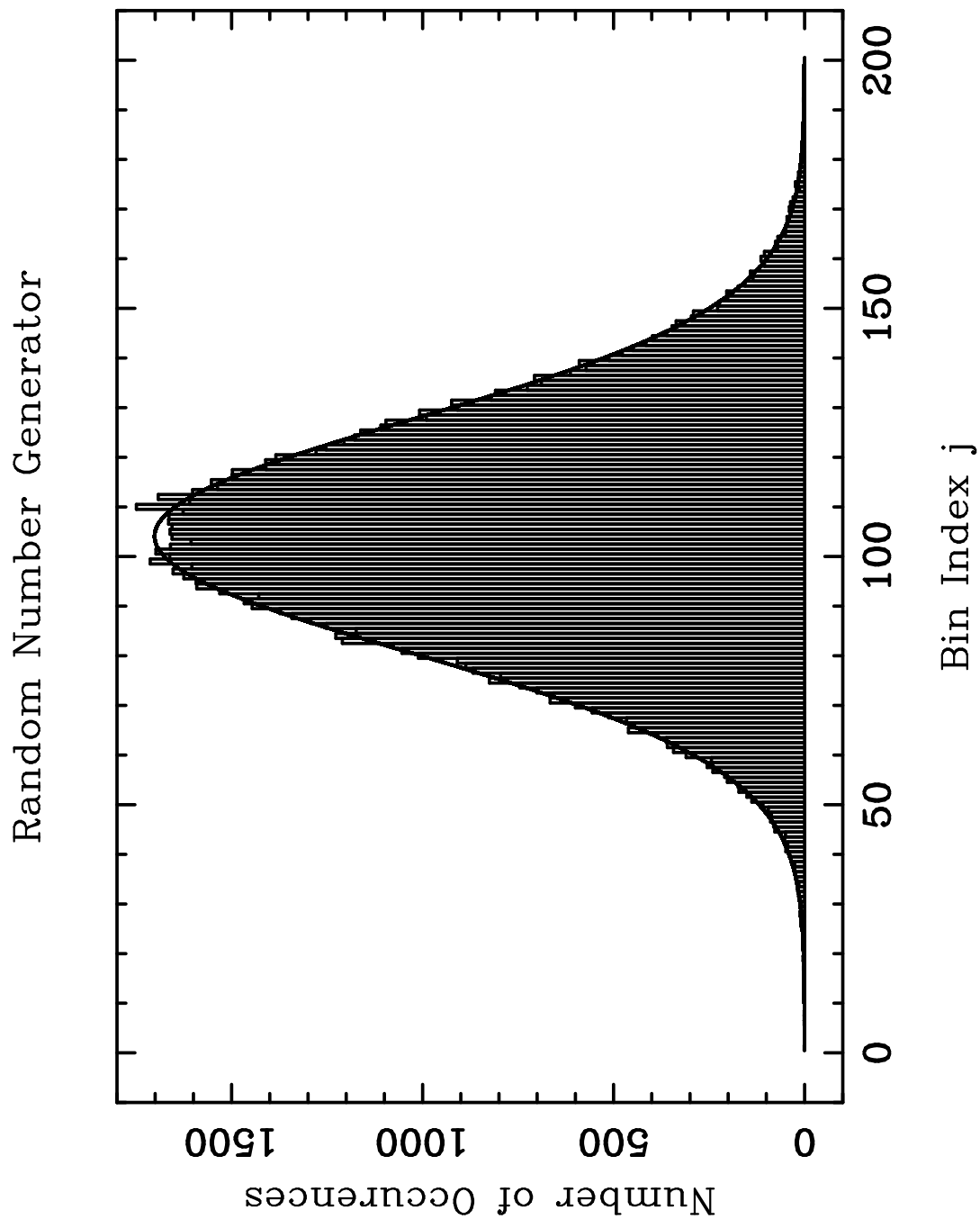


FIG. 3. Partition of the  $10^5$  values obtained using the random number generator into 200 bins as described in the text. The solid line is a Gaussian fit.

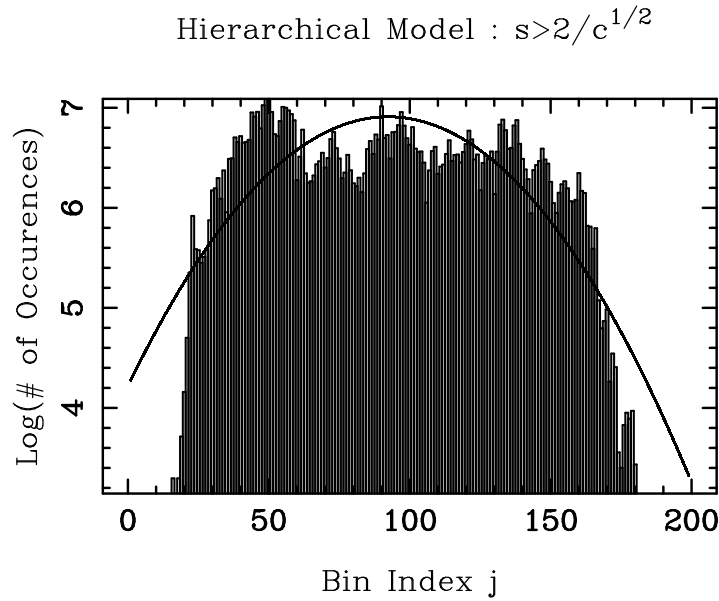
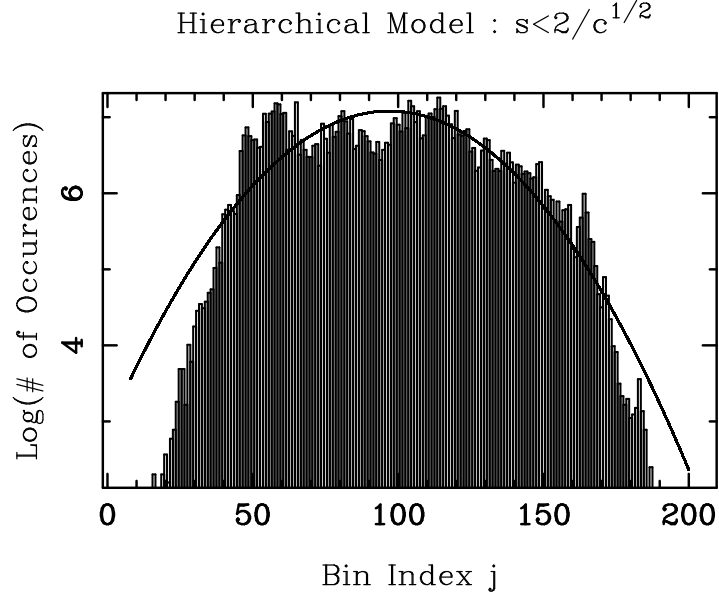


FIG. 4. Partition of the  $10^5$  values of  $\chi(s)$  for  $s < 2/\sqrt{c}$  and  $10^5$  values for  $s > 2/\sqrt{c}$  into 200 bins, for the hierarchical model. The logarithm of the number of data points in each bin is plotted versus the bin number. The solid parabola is a Gaussian fit.

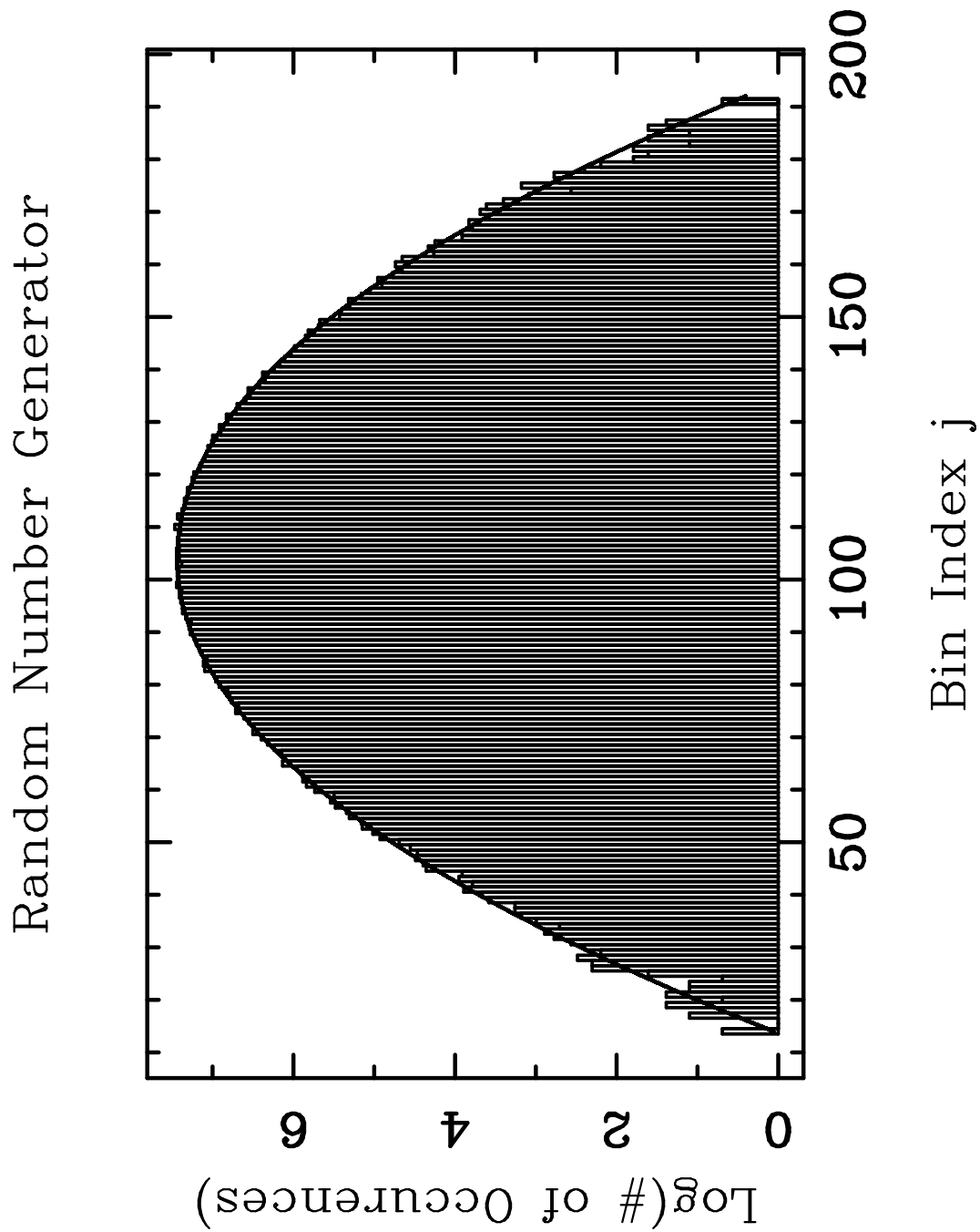


FIG. 5. Partition of the  $10^5$  values obtained from the random number generator described in the text into 200 bins. The logarithm of the number of data points in each bin is plotted versus the bin number. The solid parabola is a Gaussian fit.

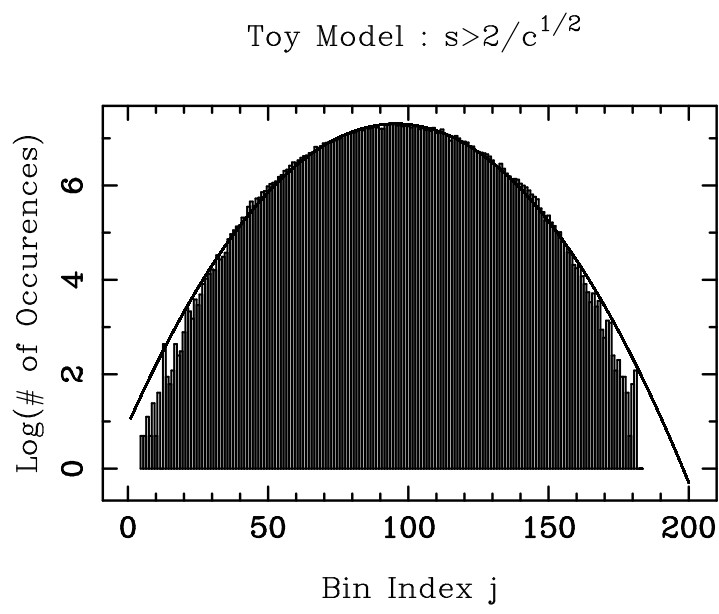
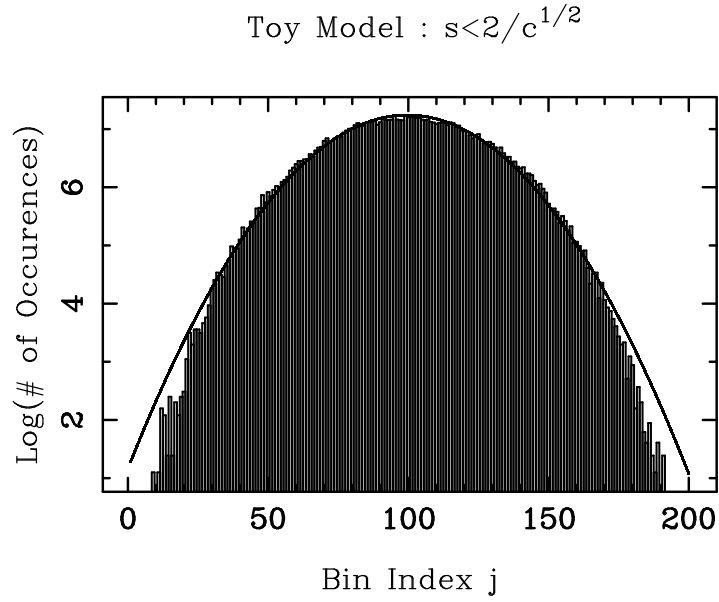
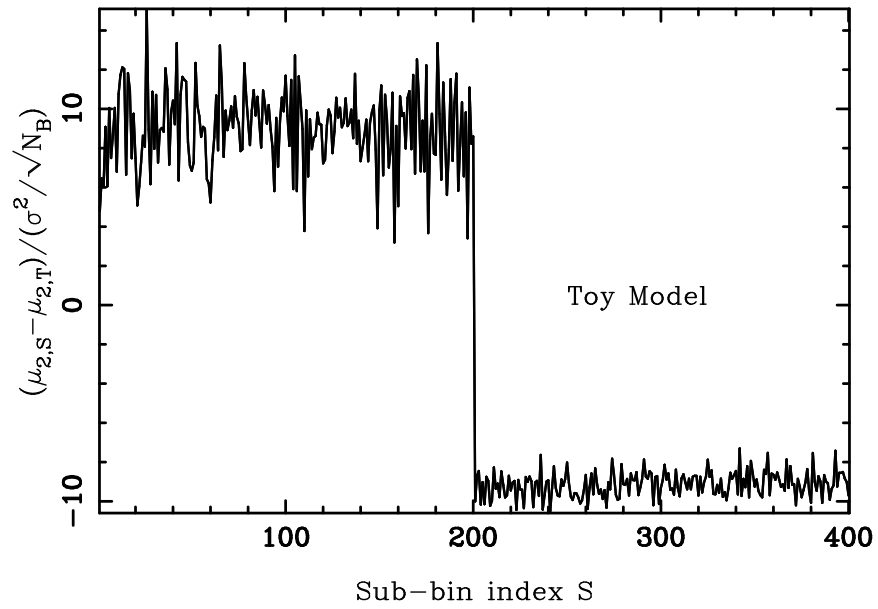
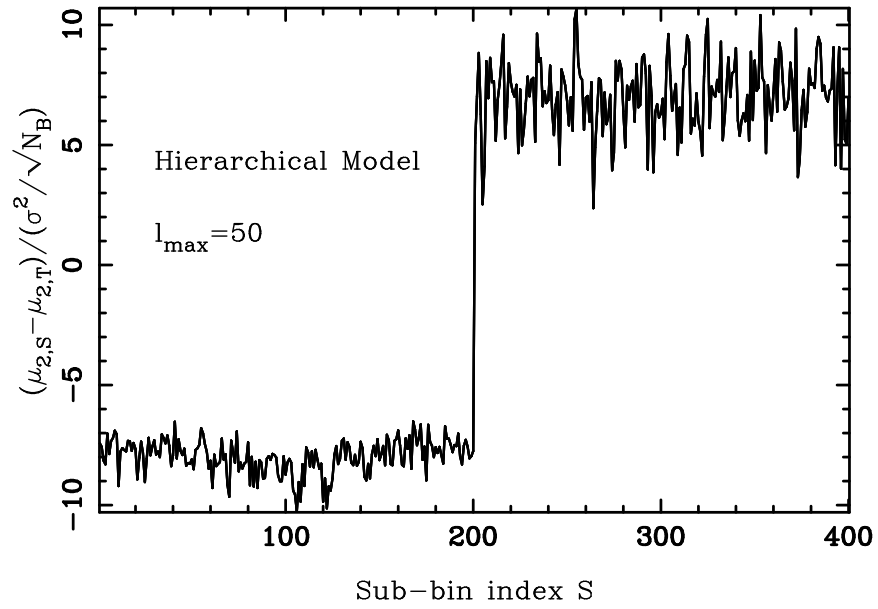


FIG. 6. Partition of the two sets of  $10^5$  values described in subsection IV B into 200 bins, for the toy model. The logarithm of the number of data points in each bin is plotted versus the bin number. The solid parabola is a Gaussian fit.





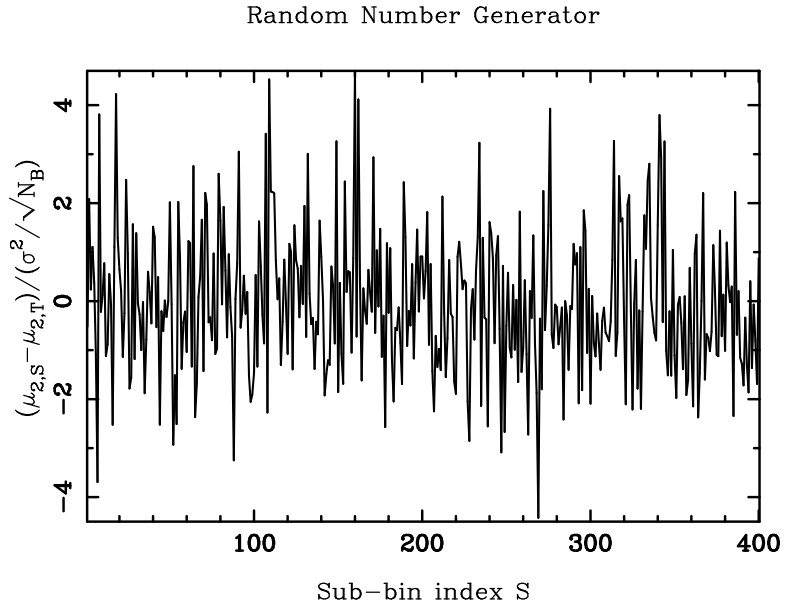


FIG. 7.  $(\widehat{\mu}_{r,S} - \widehat{\mu}_{r,T}) / (\sigma^2 / \sqrt{N_B})$  for 400 sub-bins indexed by  $S$  as explained in the text, for the three sets previously abbreviated as H.M.a.+b., T.M.a.+b. and R.N.G.

TABLES

TABLE I.  $\mu$  and  $\sigma$  for the 7 sets of data considered

	H.M.(a.+b.)	H.M.a.	H.M.b.	T.M.(a.+b.)	T.M.a.	T.M.b.	R.N.G.
$\mu$	1045	1297	803	-3037	-3023	-3029	4.22
$\sigma$	2123	2561	1524	3163.00	2062	3967	4149

TABLE II. Values of the  $p_i$  for the seven sets of data considered.

	H.M.(a+b)	H.M.a.	H.M.b.	T.M.(a+b)	T.M.a.	T.M.b.	R.N.G.
p1	7.5	2.6	11	1.02	0.86	0.85	1.057
p2	41	1.16	2.0	33	1.18	0.98	0.987
p3	4.3	1.04	1.66	0.875	1.04	0.94	0.998
p4	26	1.11	1.72	15	1.20	0.95	1.018

TABLE III. Skewness and kurtosis coefficients

	H.M.(a+b)	H.M.a.	H.M.b.	T.M.(a+b)	T.M.a.	T.M.b.	R.N.G.
$\mu_3/\mu_2^{3/2}$	0.31	0.12	0.15	-0.0033	-0.0090	0.0038	-0.00048
$\mu_4/\mu_2^2 - 3$	-0.58	-1.10	-0.81	0.56	-0.29	-0.34	-0.015